

Spatial variability in carbon dioxide exchange processes within wet sedge meadows in the Canadian High Arctic

Claire M. WRIGHT, Amy C. BLASER, Paul M. TREITZ & Neal A. SCOTT*

Department of Geography and Planning, Queen's University, Kingston, Ontario, Canada, K7L 3N6

Received 15 October 2020; accepted 11 March 2021; published online 30 March 2021

Abstract Wet sedge meadows are the most productive plant communities in the High Arctic. However, the controls on carbon dioxide (CO₂) exchange processes within wet sedge communities – and the scale at which they operate – are poorly understood. Here, the factors controlling CO₂ exchange of wet sedge meadows experiencing different moisture regimes are examined. Environmental data are used to create predictive models of CO₂ exchange on multiple temporal scales. Automated chamber systems recorded CO₂ fluxes at 30-minute intervals at wet sedge sites in the Canadian High Arctic from June to August in 2014 and 2015. Static chambers were also deployed over a larger spatial extent in 2014. Our results show that wet sedge communities were strong CO₂ sinks during the growing season (–7.67 to –44.36 g C·m⁻²). CO₂ exchange rates in wetter and drier areas within wet sedge meadows differed significantly (Wilcoxon, $p < 0.001$), suggesting that soil moisture regimes within vegetation types influence net CO₂ balance. Random Forest models explained a significant amount of the variability in CO₂ flux rates over time ($R^2 = 0.46$ to 0.90). The models showed that the drivers of CO₂ exchange in these communities vary temporally. Variable moisture regimes indirectly influenced CO₂ fluxes given that they exhibit different vegetation and temperature-response characteristics. We suggest that the response of a single vegetation type to environmental changes may vary depending on microenvironment variability within that community.

Keywords High Arctic, carbon dioxide exchange, wet sedge, soil moisture

Citation: Wright C M, Blaser A C, Treitz P M, et al. Spatial variability in carbon dioxide exchange processes within wet sedge meadows in the Canadian High Arctic. *Adv Polar Sci*, 2021, 32(1): 1-19, doi: 10.13679/j.advps.2020.0033

1 Introduction

The climate is changing at an unprecedented rate at high latitudes. In the Arctic, increases in surface air temperatures are approximately double those observed at lower latitudes – a phenomenon known as Arctic amplification (Box et al., 2019; IPCC, 2019). Precipitation regimes are also shifting, with a marked increase in volume across the Arctic (Bintanja and Selten, 2014; Vihma et al., 2016) and a trend towards increased summer rainfall (Beel et al., 2020). Amplified changes in temperature and precipitation are driving secondary impacts across the Arctic such as

reductions in snow cover, earlier snowmelt, and regional increases in permafrost active layer depth (Kankaanpää et al., 2018; Mekonnen et al., 2018; Mudryk et al., 2018).

The rapid changes being experienced at high latitudes could be causing substantial alterations to the Arctic carbon cycle through the stimulation of microbial activity and changes to vegetation. As the climate warms, the permafrost carbon pool is becoming vulnerable to thaw and degradation, leading to the release of greenhouse gases through heterotrophic respiration and other processes (Schuur and Abbott, 2011; Voigt et al., 2019). On the other hand, significant increases in plant biomass have been observed in several Arctic areas (Ju and Masek, 2016; Myers-Smith et al., 2020). Arctic greening trends have been measured from satellite observations of land surface

* Corresponding author, ORCID: 0000-0002-2965-4185, E-mail: neal.scott@queensu.ca

reflectance using NDVI (normalized difference vegetation index) (Beamish et al., 2020; Myers-Smith et al., 2020). Arctic greening could play a central role in the Arctic carbon cycle by removing CO₂ from the atmosphere, thus offsetting inputs from enhanced respiration linked to warmer temperatures. Observations of increasing plant biomass have been accompanied by a shift in vegetation community structure. Numerous studies indicate an increase in the relative abundance of vascular vegetation including shrubs and graminoids in the Low Arctic (Hobbie et al., 2017; Myers-Smith et al., 2019). Although trends are more variable at higher latitudes (Sim et al., 2019; Ravolainen et al., 2020), there has been research showing an increase in vascular abundance with warming (Elmendorf et al., 2012; van der Wal and Stien, 2014). Wookey (2009) proposed that shifts in plant dominance will result in an intricate series of biotic cascades and feedbacks which will either enhance or dampen CO₂ release. Given that permafrost soils are estimated to store over 30% of all surface soil carbon (0 – 3 m) (Hugelius et al., 2014; Plaza et al., 2019), climate-induced changes to net carbon storage in the Arctic through stimulated respiration and/or changes to plant cover could have a significant impact on the global carbon budget.

Since the CO₂ budget in High Arctic landscapes is often delicately balanced, with close to zero annual net CO₂ exchange (Lüers et al., 2014), small changes to environmental variables can mean the difference between a region being a CO₂ sink or a source (Dagg and Lafleur, 2011; Treat et al., 2018). At the most basic level, primary productivity is regulated by incoming photosynthetically active radiation (PAR), as photosynthesis cannot occur in its absence. In the High Arctic, plant productivity is restricted to the summer growing season when PAR is available and air temperatures are suitable for photosynthesis to occur. Soil temperature and moisture can also influence productivity and respiration. Numerous studies have found that increasing temperature has a positive effect on heterotrophic respiration rates in the Arctic, and in some cases on gross primary production (GPP) (Lavoie et al., 2011; Natali et al., 2014, 2015). Moreover, higher rates of decomposition and ecosystem respiration (ER) have been reported for High Arctic ecosystems following increased water availability (Illeris et al., 2003; Christiansen et al., 2012; Emmerton et al., 2016). Ecosystem GPP has been observed to have a weaker response to increased temperature and soil moisture compared to ER (Marchand et al., 2005; Natali et al., 2015). Other changes driven by altered temperature and precipitation regimes, such as snow cover, active layer depth, and nutrient availability can all influence CO₂ fluxes (Lavoie et al., 2011; Cannone et al., 2019; Ravn et al., 2020). There is clearly a delicate balance between key biophysical variables and growing season CO₂ exchange rates that influence whether Arctic ecosystems are a source or sink of CO₂.

Large scale predictions of Arctic CO₂ fluxes are

further complicated by the heterogeneity of vegetation across the landscape resulting from variation in soil moisture regimes (Atkinson et al., 2020). Indeed, Treat et al. (2018) found that landscape scale variation among tundra vegetation types exerted much greater control over decadal CO₂ fluxes (net ecosystem exchange; NEE) than inter-annual climate variability. The study also determined that the net regional carbon balance relied on the relative abundance of uplands versus wetlands. Wetlands are of particular interest in the Arctic because they tend to be strong CO₂ sinks (Emmerton et al., 2016; Sim et al., 2019). Accordingly, research suggests that wet sedge meadows are net CO₂ sinks in the High Arctic (Welker et al., 2004; Kwon et al., 2006; Atkinson et al., 2020). The carbon storage capacity of wetlands makes Arctic wet sedge communities a vegetation type of particular significance. Importantly, High Arctic wet sedge communities have been shown to have a long-term positive response to climate warming in terms of biomass, decomposition, and productivity (Hill and Henry, 2011). Wet sedge meadows generally occur in low-lying areas proximal to waterways or permafrost snow fields and are characterized by a thick layer of grasses (e.g., *Alopecurus alpinus*, *Phippsia algida*), sedges (e.g., *Carex aquatilis* var. *stans*, *Eriophorum triste*, *E. scheuchzeri*) and mosses (Liu and Treitz, 2016). Although they are considered more spatially homogeneous than other High Arctic vegetation types in terms of species composition, sedge meadows are subject to a strong moisture gradient with significant variation observed in percent cover and biomass (Webber, 1978; Atkinson and Treitz, 2013). Though some previous studies have recognized that multiple moisture classes exist within High Arctic sedge meadows (Liu and Treitz, 2016; Campbell et al., 2020), little is known about differences in CO₂ exchange processes within spatially variable wet sedge communities.

In this study, we examined growing season CO₂ exchange within wet sedge communities in the Canadian High Arctic. We used a combination of static CO₂ chambers deployed over a larger area with approximately bi-weekly measurements and autochambers set up locally with constant half-hourly measurements. Our objectives were: (1) to compare CO₂ fluxes and their controls between wet sedge meadows under different moisture regimes; and (2) to examine the performance of various models for predicting CO₂ fluxes at different temporal scales in High Arctic wet sedge communities.

2 Methods

2.1 Site description and field sampling

This research was conducted at the Cape Bounty Arctic Watershed Observatory (CBAWO) (Figure 1) located on the southern coast of Melville Island, Nunavut (74°54'N, 109°35'W). It is in continuous permafrost, with a 0.5 to 1 m

thick active layer. The growing season lasts from roughly mid-June to mid-August (Hung and Treitz, 2020). The mean summer air temperature (June to August) at the CBAWO is 2.7 ± 1.4 °C (2003–2017) (Beel et al., 2020). The landscape is dominated by three major vegetation types: polar

semi-desert, mesic tundra, and wet sedge meadows (Atkinson and Treitz, 2012). Wet sedge meadows at the CBAWO tend to be in low-lying areas near a continuous water supply (e.g., semi-permanent snowfields) (Woo et al., 2006; Thompson and Woo, 2009).

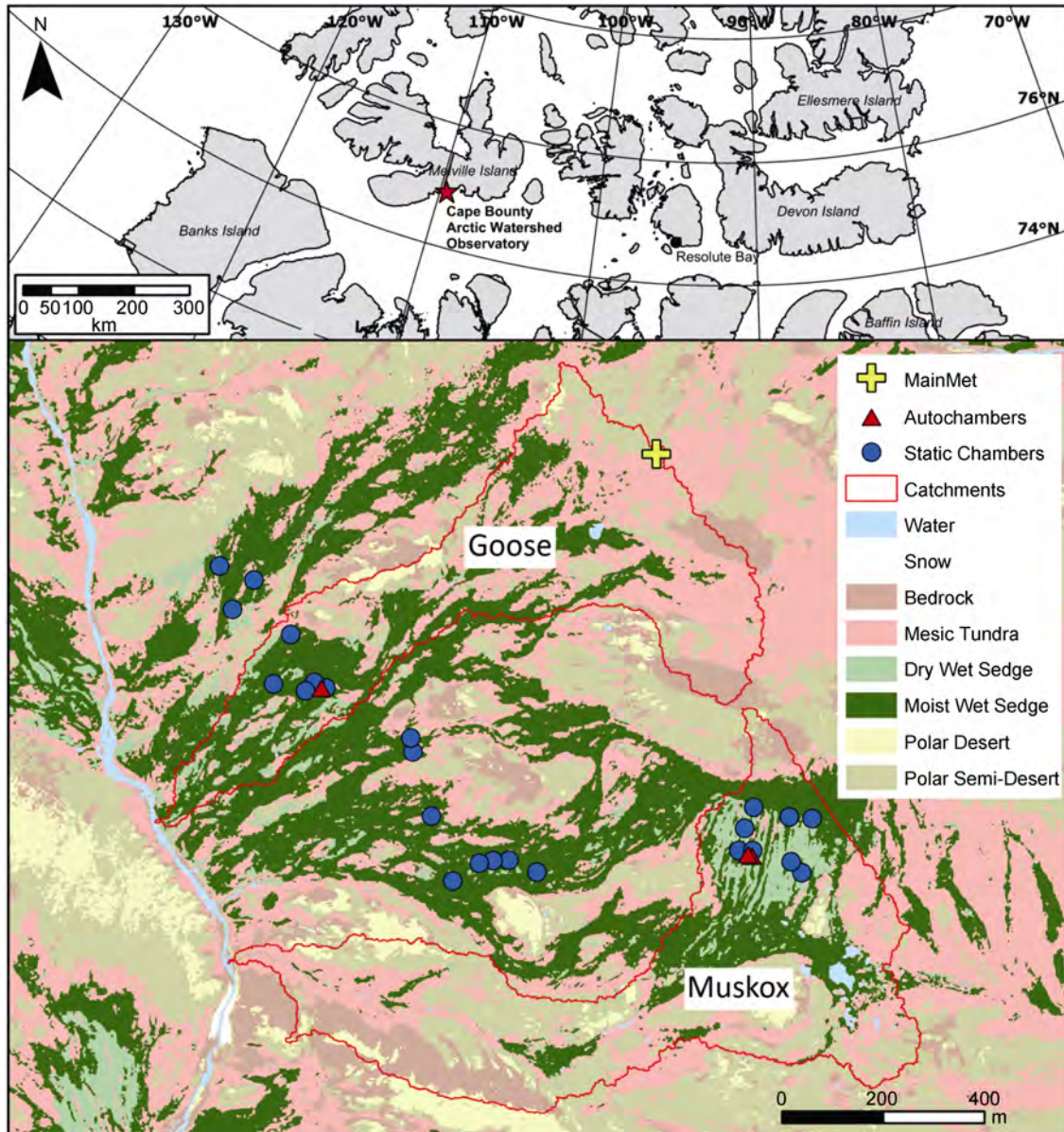


Figure 1 Map showing autochamber and static chamber positions on Melville Island (inset) and Cape Bounty Arctic Watershed Observatory site (red star) in the Canadian High Arctic. Catchments were generated using the SWAT hydrological modelling tool (Arnold et al., 2012).

In preparation for this work, a plant community classification for the CBAWO was derived based on spectral analysis of Worldview-2 imagery acquired in July 2012 (Nanfeng Liu, pers. comm.). This classification has subsequently been formalized for the CBAWO using WorldView-2 data collected in 2018 (Hung and Treitz, 2020). The initial supervised (*k*-means) classification resulted in five spectrally distinct classes of landscape vegetation cover:

polar semi-desert, mesic tundra (dry and wet), and wet sedge meadow (dry and wet). Wet sedge meadows accounted for a total of 16.6% of the CBAWO area with 14.5% of the area being classified as moist wet sedge. The dry and wet sub-categories provide a more precise representation of soil moisture gradients at the CBAWO compared to previous classifications (Liu and Treitz, 2016). *In situ* measurements acquired at the beginning of the sampling season confirmed

that the volumetric water content at 7 cm depth was greater than 60% at wet sites and less than 60% at dry sites. The designation of wet and dry sub-classes for wet sedge vegetation provided an opportunity to investigate CO₂ dynamics along a moisture gradient within this community type.

Using this new classification combined with past knowledge of the study site, three large plots (300 m × 300 m each) were delineated across the landscape. Each plot contained all three of the major vegetation types, as well as both wet sedge subcategories (i.e., wet sedge (dry) and wet sedge (wet)). The three large plots together aimed to capture spatial variation by covering the spectrum of wet sedge meadow sites at the CBAWO. Within each plot, eight sample sites were identified containing both wet sedge (dry) and wet sedge (wet) vegetation types. A collar (20 cm diameter by 15 cm high) for static chamber CO₂ measurements was installed at each location. Automated Soil CO₂ Exchange Systems (ACE: ADC Bioscientific Ltd., Hertfordshire, UK) were installed in two plots only (one pair in the Goose catchment, and two pairs in the MuskoX catchment; Figure 1). Environmental measurements occurred within the three plots except air temperature and precipitation, which were collected at the nearby ‘Main Met’ meteorological station (Beel et al., 2020) equipped with a shielded Onset temperature and relative humidity sensor 1.5 m above ground surface (± 0.2 °C; 5% RH), and an Onset tipping bucket precipitation gauge (0.2 mm tip), logged hourly with an Onset U30 logger (Onset Computer Corporation, Bourne, MA, USA).

Once on-site at the CBAWO in 2014, collar locations were adjusted visually and confirmed with *in situ* soil moisture measurements. Some sampling sites installed during snowmelt were redistributed after snowmelt was complete to conform to the appropriate vegetation type designation. This resulted in 16 wet sedge (wet) and 8 wet sedge (dry) static chamber collars spread throughout the three plots. Although it was originally planned to sample an even number of each, the updated site locations more accurately represent the larger proportion of wet sedge (wet) areas within the plots and at the CBAWO.

2.2 Environmental measurements

Environmental measurements (e.g., soil moisture and temperature) were collected in conjunction with static and autochamber CO₂ measurements. At the static chamber sites, measurements were taken approximately every 4 d. Soil moisture was measured with a ML2 Thetaprobe (±0.05 m³·m⁻³, range 0 to 70 °C) and HH2 Moisture Meter Logger (Delta T Devices Ltd., Cambridge, UK) to a depth of 7 cm, and soil temperature was measured at 5 cm and 10 cm depths with a digital thermometer (Taylor model 9878E, ±2.5 °C; range -40 to 260 °C) (Taylor Precision Products Inc., Oak Brook, IL, USA). At the autochamber sites, soil moisture measurements were collected every 30 min using buried 10HS and EC-5 Soil Moisture Sensors (±0.03 m³·m⁻³;

0 to 50 °C) and ECH2O loggers (Decagon Devices, Pullman, WA, USA). Soil temperature measurements were collected every 30 min using buried HOBO Pro V2 soil temperature sensors (±0.21 °C; range -40 to 70 °C) with external sensor cables (Onset Computer Corporation, Bourne, MA, USA) at 5 and 10 cm depths. Each pair of ACE units had a corresponding moisture and temperature probe located adjacent to the unit. PAR (μmol·m⁻²·s⁻¹) was collected by the transparent ACE units in conjunction with each half-hourly CO₂ measurement. Air temperature was based on hourly data from the nearby meteorological station (Main Met).

2.3 NDVI measurements

Digital photographs of each sampling site were collected using the Canon 650NDVI (T4i NDVI) digital camera with three spectral bands: blue, green, and near-infrared (Maxmax Inc., Carlstadt, NJ, USA). Photographs were taken of quadrats (0.5 m × 0.25 m) adjacent to each static chamber collar in the three large plots. No more than one day separated static CO₂ measurements and the acquisition of NDVI photographs (i.e., a photograph was taken on average every 4 d). NDVI images were collected between 1000 and 1600 to minimize solar zenith angle effects and to ensure consistent light conditions. Images were collected approximately 150 cm above the canopy, with a bubble level to ensure the camera lens remained horizontal, and with consistent camera settings (i.e., manual exposure program).

The traditional NDVI formula uses the reflectance (*R*) of the NIR and red bands, while the Canon 650NDVI uses NIR and either green or blue (G/B) for the calculation. Those RGB bands can be reliably substituted since the calculation still uses a NIR plant reflective channel and a visible plant absorption channel (Maxmax Inc., Carlstadt, NJ, USA). In this case, NDVI was derived using reflectance in the near infrared and blue bands (Equation 1). It has been widely argued that this method is at least five times more sensitive to chlorophyll-*a* content than traditional NDVI, and that it is especially useful for differentiating stressed and senescent vegetation (Gitelson et al., 1996), an important distinction in these wet sedge communities. All NDVI measurements within the same plot and moisture designation (wet or dry) were averaged on a given date. For modelling purposes, the NDVI values for the nearest static chamber were attributed to each autochamber.

$$NDVI = \frac{R_{NIR} - R_B}{R_{NIR} + R_B} \quad \text{Equation 1}$$

2.4 CO₂ flux measurements

Static chamber measurements were carried out in 2014 using methods described by Beamish et al. (2014). Briefly, a round transparent chamber (~ 9 L volume) outfitted with a Vaisala GMP343 Carbon Dioxide Probe and temperature/relative humidity sensor (Vaisala HMP75) (Vaisala, Helsinki, Finland) was used to measure net ecosystem exchange (NEE) of CO₂ at each collar. The chamber was returned to ambient

CO₂ concentrations after each measurement. After measurement of NEE, ER was measured by placing an opaque cover over the chamber. Both NEE and ER were determined by measuring chamber CO₂ concentration changes over a 5-min period. Measurements of atmospheric pressure necessary for subsequent gas concentration conversions were taken in conjunction with these chamber measurements using a Kestrel 3500 Wind Meter (± 1.5 hPa·m⁻¹) (Nielsen-Kellerman Co., Boothwyn, PA, USA). All measurements were taken during the day between 1000 and 1600 in order to consistently capture daily maximum incoming solar radiation. Static chamber fluxes were measured approximately every 4 d in July leading to six values per chamber.

Three pairs of ADC ACE autochambers were deployed to collect flux data throughout the 2014 and 2015 growing seasons at the CBAWO. Although the low number of chambers meant that replicate measurements were limited, previous work at the same site has shown that fluxes remain consistent for adjacent autochamber pairs. Two pairs of chambers (i.e., two transparent and two opaque) were

installed at Muskox – one pair each in wet sedge (wet) and wet sedge (dry) locations. One pair was installed in the Goose catchment at a wet sedge (wet) site. Metal collars (20 cm dia.) were installed in the soil at each sampling location at the beginning of the season, onto which the chambers were clamped for the duration of the sampling period. Autochambers were powered by a 12 V battery attached to two 30W solar panels (Solartech Power Inc., Anaheim, CA, USA). Battery voltage was checked weekly to ensure adequate power to the ACE units. NEE was measured in the units equipped with transparent lids, and ER in the units equipped with an opaque lid (Figure 2). Measurements occurred every 30 min, for a period of 3 min (CO₂ concentration measured every 10 s), in closed mode with open ‘zero’ measurement following each cycle to reset the system to ambient CO₂ prior to each measurement (ADC BioScientific Ltd, 2009). Approximately 2000 measurements were collected by each chamber throughout the growing season. Data were collected weekly to assess data quality and instrument performance.



Figure 2 Pair of ADC ACE autochambers installed in the Muskox catchment site at the Cape Bounty Arctic Watershed Observatory taken by Dr. Neal Scott in 2017; transparent (right) and opaque (left).

2.5 Static chamber data processing

Static chamber CO₂ concentrations (ppm) were converted to $\mu\text{mol}\cdot\text{m}^{-3}$ using Equation 2:

$$C(\mu\text{mol}\cdot\text{m}^{-3}) = C(\text{ppm}) \times \frac{P(\text{hPa})}{R \times T(\text{K})} \quad \text{Equation 2}$$

where $T(\text{K})$ is the average of the first and last interior chamber temperatures, $P(\text{hPa})$ is the atmospheric pressure, and R is the ideal gas constant ($0.08314 \text{ hPa}\cdot\text{m}^{-3}\cdot\text{mol}^{-1}\cdot\text{K}^{-1}$). To eliminate sampling artifacts (i.e. the mixing period when the chamber is first closed), the first four readings (1 min)

were removed prior to analysis (Kutzbach et al., 2007; Heinemeyer et al., 2011). Flux rates were then calculated by taking a linear regression of CO₂ concentration over time. Flux measurements were converted to units of $\mu\text{mol}\cdot\text{m}^{-2}\cdot\text{s}^{-1}$ using Equation 3:

$$\text{Flux} = S(\mu\text{mol}\cdot\text{m}^{-3}\cdot\text{s}^{-1}) \times \frac{V(\text{m}^3)}{A(\text{m}^2)} \quad \text{Equation 3}$$

where S is the slope, V is the total chamber volume, and A is the ground area within the collar. Flux calculations resulted in one flux value for each five-minute measurement period.

2.6 Autochamber data processing

Output files for each autochamber reading provided a Reference CO₂ value ($\mu\text{mol}\cdot\text{m}^{-3}$), a Delta CO₂ value ($\mu\text{mol}\cdot\text{m}^{-3}$), and a Net CO₂ Exchange Rate (NCER) value ($\mu\text{mol}\cdot\text{m}^{-2}\cdot\text{s}^{-1}$). Reference values represent an estimate of ambient CO₂ concentrations at the start of each reading; Delta CO₂, the difference between Reference CO₂ and the final CO₂ concentration in the chamber; and NCER, the calculated net CO₂ exchange rate. However, due to the exponential regression employed by ADC for NCER calculations, negative fluxes (representing net uptake of CO₂) could not be calculated and were automatically truncated to zero. One ACE unit, however, had updated software which provided an output file with the raw 10-second CO₂ measurements for every cycle, as well as the pre-calculated values noted above. These data were invaluable to develop and test a method for calculating negative flux values.

For five of the ACE units, in the case of missing or negative NCER values, Delta CO₂ values (final CO₂ – Reference CO₂) in $\mu\text{mol}\cdot\text{m}^{-3}$ were used to derive new NCER values (Equation 4). For the lone chamber that provided all the raw measurements, a linear regression was used to calculate the Delta (flux) value using the slope of the change in concentration over time (similar to static chamber flux calculations). This method, based on the full data, yielded almost identical NCER estimates as those using the more limited Delta CO₂ values, with occasionally slightly smaller amplitudes in the diel fluxes. This gave confidence that the two methods were providing comparable results.

$$NCER = \Delta\text{CO}_2 (\mu\text{mol}\cdot\text{m}^{-3}) \times \frac{V(\text{m}^3)}{A(\text{m}^2)} / T(\text{s}) \times 1000 (\mu\text{mol}\cdot\text{mol}^{-1})$$

Equation 4

Next, data outliers were identified using a procedure modified from Savage et al. (2008). First, a visual inspection was performed to identify suspect NCER values. NCER values with a magnitude greater than $25 \mu\text{mol}\cdot\text{m}^{-2}\cdot\text{s}^{-1}$ were removed as these were assumed to be erroneous.

After establishing that the data were non-parametric (Shapiro-Wilks test, $p < 0.001$; Levene's test, $p < 0.001$), a two-part filter was applied to identify outliers. First, a median absolute deviation (MAD) value was calculated using Equation 5.

$$MAD = b \times \text{median}(|x_i - \text{median}(x)|)$$

Equation 5

The consistency constant (b) was calculated as the inverse of the 75th quantile since the underlying distribution was not normal (Leys et al., 2013). Suspect fluxes were then identified using a rejection criterion of 3.5 (Equation 6). A conservative threshold was chosen due to the variability of the data.

$$\frac{x_i - \text{median}(x)}{MAD} > \pm 3.5$$

Equation 6

Of the identified suspect fluxes, those that differed by

more than $2.5 \mu\text{mol}\cdot\text{m}^{-2}\cdot\text{s}^{-1}$ from adjacent fluxes were removed.

Overall, 8.19% of the 2014 NCER measurements and 5.20% of the 2015 NCER measurements were removed. Notably, as a result of the filtering criteria, 50.0% and 37.2% of the data were removed for the opaque autochamber at the Goose site in 2014 and 2015, respectively. Therefore, subsequent analyses were performed both with and without the Goose chamber pair. While the autochambers acquired CO₂ flux measurements on a half-hourly basis, measurements did not always align between the different units, so the data were aggregated to an hourly timescale to more accurately calculate GPP after filtering was complete. GPP was calculated as the difference between NEE (NCER for transparent chambers) and ER (NCER for opaque chambers).

2.7 Random Forest (RF) modelling

Random Forest (RF) regression modelling of the three CO₂ fluxes was carried out using the 2014 autochamber data. PAR, air temperature, soil temperature (5 and 10 cm depths), and soil moisture (5 and 10 cm depths) were included as environmental variables. Some models were also run with Julian Day and/or with a categorical soil moisture designation for wet and dry sites. The 2014 data were split into a training dataset (70%) and a validation dataset (30%) using a random sub-setting algorithm. A RF regression was performed using the Party package in R (Hothorn et al., 2020). The algorithm used was conditional inference RF modelling which helps to reduce bias and the risk of overfitting compared to traditional RF (Hothorn et al., 2006). The number of variables randomly available for each node in each decision tree (mtry) was set to 3 following the rule of $\text{mtry} = \frac{p}{3}$ where p is the number of predictive variables (Hastie et al., 2017). The number of trees used in each modelling run (ntree) was set to 1000. This was judged sufficient as the results of the model did not differ systematically when the random seed was changed (Strobl et al., 2008).

The 2014 data were modelled first without Julian Day or Moisture designations, and then with each to determine their relative importance. Then, the impact of the environmental variables was evaluated using the varImp() function from the Party package. VarImp() uses permutation importance in order to eliminate bias introduced by the high amount of collinearity existing between predictive variables (Strobl et al., 2008). The accuracy of the prediction was tested using the validation dataset based on root mean square error (RMSE) and R^2 values derived using the Caret package in R (Kuhn et al., 2020). The R^2 values were calculated as the square of the correlation between the observed and predicted outcomes. The model was also tested against one pair of autochambers from the 2015 dataset. Finally, the data were modelled at daily and weekly timescales to assess changes in variable importance. Daily flux values were

calculated as a simple average of hourly values for each date. Meanwhile, weekly values were calculated using a 7-day moving average.

2.8 Respiration models

The RF model for respiration was compared with several traditional ER models. While a wide range of respiration models have been developed and tested in temperate ecosystems, few have been evaluated with direct measurements of ecosystem respiration in the High Arctic. ER is typically approximated using CO₂ flux measurements made during periods of darkness, but this option is not available in the High Arctic during the growing season. Therefore, respiration is generally modelled rather than measured directly. We tested a number of commonly used respiration models (based on Richardson et al., 2006) by comparing measured and predicted values using nonlinear least squares estimates from the `nls()` function in the *R* base package. Model starting parameters were estimated based on literature values.

3 Results

3.1 Climate

Both 2014 and 2015 had cooler summers (June 1st to August 31st) compared to a ten-year average (2005 to 2015) of growing season air temperature measured at the Main Met station for the CBAWO. The average air temperature from June to August was 1.66 °C in 2014 and 3.07 °C in 2015. In both years, air temperature increased from the beginning of June to mid-July, underwent a brief period of cooling, and then remained relatively constant for all of August (Figure 3). The total precipitation in 2014 (37 mm) was similar to the 2005–2015 growing season average measured at Main Met, while the 2015 growing season experienced significantly higher levels of rainfall (102 mm) (Figure 3). Precipitation was mainly concentrated in late July for 2014. By contrast, in 2015, rainfall events occurred throughout the summer season.

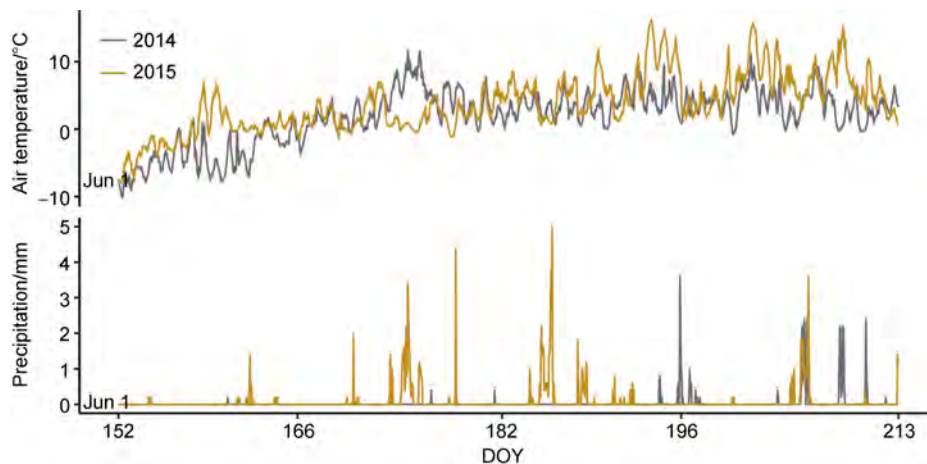


Figure 3 Average daily air temperature and precipitation recorded at the main meteorological station at the Cape Bounty Arctic Watershed Observatory from June 1st to August 31st in 2014 and 2015. DOY = Day of the Year.

3.2 Environmental variables and CO₂ fluxes

Automated soil moisture measurements at the three autochamber sites in 2014 confirmed that dry sites had significantly lower levels of soil moisture (30% – 50% drier) compared to wet sites at 5 and 10 cm depths (Wilcoxon $p < 0.001$). Average air temperature and PAR did not differ between wet and dry sites in either year (Wilcoxon $p > 0.1$). As well, there was no significant difference in soil temperature readings between wet and dry sites in 2014. However, soil temperatures were significantly cooler at wet sites compared to dry sites at both 5 and 10 cm depths in 2015 (Wilcoxon $p < 0.001$). NDVI measurements using the NIR and blue bands differed significantly between the wet and dry sites (Wilcoxon $p < 0.01$). In both years, hourly ER was most

strongly correlated with soil temperature measured at 5 cm depth followed by soil temperature at 10 cm depth and air temperature (Table 1). GPP and NEE were most strongly correlated with PAR except GPP in 2014 which had the highest correlation with soil temperature at 5 cm depth. ER had low correlation with PAR. Correlation for all fluxes with soil moisture was low in 2014 (not measured in 2015).

3.3 Autochamber CO₂ fluxes

The three autochamber locations exhibited a clear diel pattern for all fluxes (Figure 4). Growing season median ER using all autochamber data was $0.67 \pm 0.49 \mu\text{mol}\cdot\text{m}^{-2}\cdot\text{s}^{-1}$ in 2014 and $0.93 \pm 0.61 \mu\text{mol}\cdot\text{m}^{-2}\cdot\text{s}^{-1}$ in 2015. For GPP, median flux values were $-1.00 \pm$

Table 1 Pearson linear correlation coefficients between hourly carbon dioxide fluxes and environmental variables measured at the Cape Bounty Arctic Watershed Observatory for the 2014 and 2015 summer season. Soil moisture was not measured in 2015

	2014			2015		
	ER	GPP	NEE	ER	GPP	NEE
PAR/($\mu\text{mol}\cdot\text{m}^{-2}\cdot\text{s}^{-1}$)	0.06	-0.38	-0.35	0.12	-0.67	-0.65
Air temperature/ $^{\circ}\text{C}$	0.33	-0.38	-0.20	0.42	-0.33	-0.13
Soil temperature 5 cm/ $^{\circ}\text{C}$	0.44	-0.50	-0.20	0.74	-0.40	-0.07
Soil temperature 10 cm/ $^{\circ}\text{C}$	0.36	-0.41	-0.17	0.57	-0.18	0.10
Soil moisture 5 cm/($\text{m}^3\cdot\text{m}^{-3}$)	0.15	0.05	0.10	-	-	-
Soil moisture 10 cm/($\text{m}^3\cdot\text{m}^{-3}$)	0.15	0.07	0.12	-	-	-

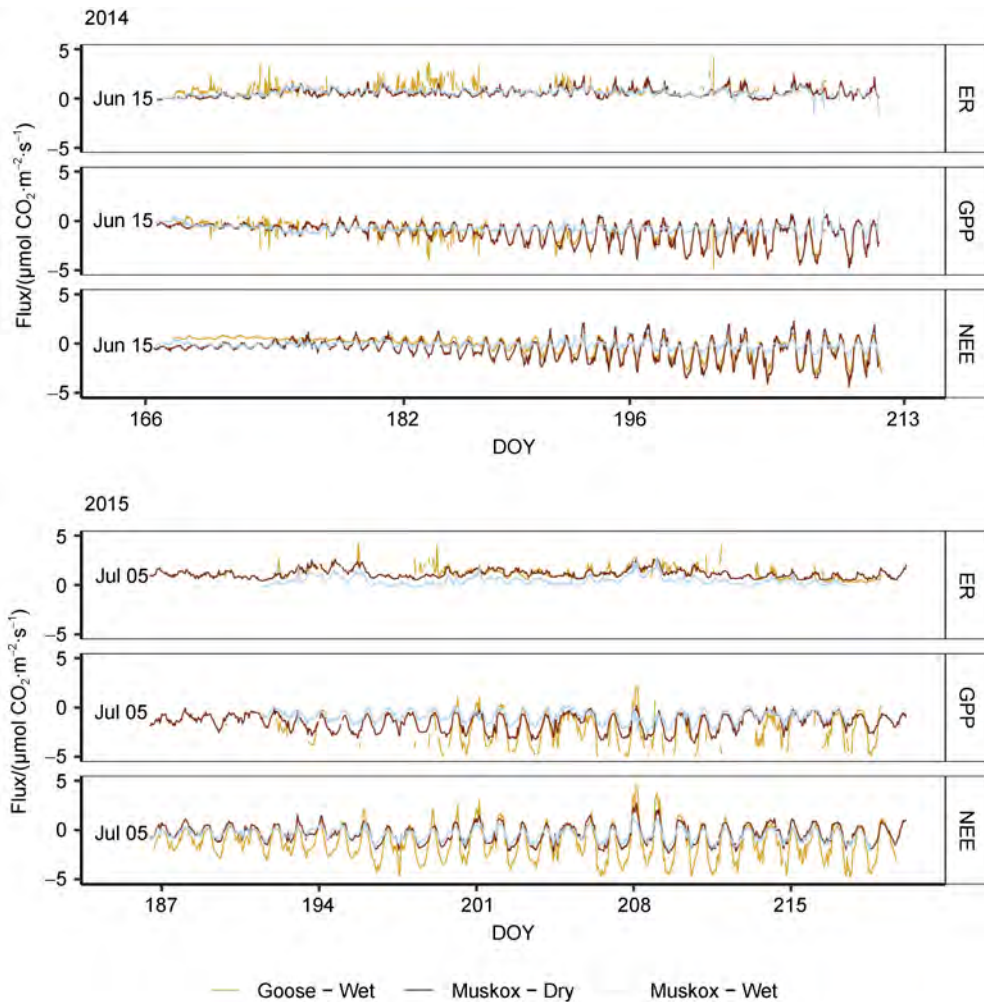


Figure 4 Hourly carbon dioxide fluxes from three autochamber pairs at the Cape Bounty Arctic Watershed Observatory for the 2014 and 2015 summer seasons (ER – Ecosystem Respiration, GPP – Gross Primary Productivity, NEE – Net Ecosystem Exchange). DOY = Day of the Year.

$0.85 \mu\text{mol}\cdot\text{m}^{-2}\cdot\text{s}^{-1}$ and $-1.6 \pm 1.2 \mu\text{mol}\cdot\text{m}^{-2}\cdot\text{s}^{-1}$ in 2014 and 2015, respectively. An overall uptake of CO_2 was observed in both years, with median NEE values of $-0.31 \pm 0.86 \mu\text{mol}\cdot\text{m}^{-2}\cdot\text{s}^{-1}$ and $-0.7 \pm 1.2 \mu\text{mol}\cdot\text{m}^{-2}\cdot\text{s}^{-1}$ in 2014 and 2015, respectively. NEE values fluctuated around zero, and the amplitude (magnitude of flux) increased as the season progressed. This trend was especially pronounced

in 2014.

Flux rates differed between wet and dry sites in both 2014 and 2015 (Table 2). In 2014, the median rate of ER was significantly lower at dry sites compared to wet sites (Wilcoxon $p < 0.001$). Meanwhile, rates of GPP and NEE were higher (i.e. more negative) at dry sites compared to wet sites (Wilcoxon $p < 0.01$). The opposite trends were

observed in 2015, with higher ER rates, and lower GPP and NEE rates at dry sites compared to wet sites (Wilcoxon $p < 0.001$). These results were not significant for GPP using the full dataset (Wilcoxon $p > 0.1$). Cumulative flux results indicate a difference between wet and dry sites (Figure 5). In 2014, both the wet sites had lower cumulative NEE (-7.67 to -7.77 g C·m⁻²) than the dry site (-27.02 g C·m⁻²). By contrast, in 2015, both the wet sites had higher cumulative NEE (-14.95 to -44.36 g C·m⁻²) compared to the dry site (-12.7 g C·m⁻²).

3.4 RF flux modelling

2014 hourly CO₂ fluxes were modelled using RF regressions with the environmental variables collected at each site (i.e., air temperature, PAR, soil temperature, soil moisture). NEE, GPP, and ER were modelled separately and validated with

30% of 2014 measurements not used to train the model. The models captured the diel pattern of the fluxes; however, for ER, the peaks in both directions were underestimated (Supplementary Figure 1). The data from the Goose site were included since model performance and results varied little with their exclusion. Based on validation with 30% out-of-bag observations, NEE and GPP had the strongest relationships with the model variables ($R^2 = 0.90$ and 0.87 , respectively) while ER had a weaker relationship ($R^2 = 0.46$) (Table 3). The results show that the models were improved by the inclusion of Julian Day based on the R^2 value. As well, the models for GPP and NEE were improved with the inclusion of a moisture designation (wet and dry). However, the addition of NDVI to the RF models greatly decreased their performance. Therefore, Julian Day and moisture designations but not NDVI were included in the analysis.

Table 2 Wilcoxon test results for median \pm absolute deviation carbon dioxide flux rates between wet and dry site designations from autochamber measurements at the Cape Bounty Arctic Watershed Observatory for the 2014 and 2015 summer seasons

	2014			2015		
	Median flux/($\mu\text{mol}\cdot\text{m}^{-2}\cdot\text{s}^{-1}$)		p -value	Median flux/($\mu\text{mol}\cdot\text{m}^{-2}\cdot\text{s}^{-1}$)		p -value
	Wet	Dry		Wet	Dry	
ER (Full)	0.66 ± 0.38	0.50 ± 0.38	< 0.001	0.63 ± 0.64	1.08 ± 0.41	< 0.001
ER (No Goose)	0.60 ± 0.33	0.50 ± 0.38	< 0.001	0.36 ± 0.42	1.08 ± 0.41	< 0.001
GPP (Full)	-0.77 ± 0.41	-0.79 ± 0.76	< 0.01	-1.2 ± 1.1	-1.37 ± 0.99	> 0.1
GPP (No Goose)	-0.76 ± 0.29	-0.79 ± 0.76	< 0.001	-0.90 ± 0.65	-1.37 ± 0.99	< 0.001
NEE (Full)	-0.06 ± 0.50	-0.39 ± 0.82	< 0.001	-0.6 ± 1.1	-0.4 ± 1.1	< 0.001
NEE (No Goose)	-0.11 ± 0.29	-0.39 ± 0.82	< 0.001	-0.38 ± 0.64	-0.4 ± 1.1	< 0.05

Note: Results for Dry sites are the same each year as there was no Dry site at the Goose site, only a Wet site.

Table 3 Model performance for Random Forest regressions of a random subset of the 2014 data collected at autochamber sites at the Cape Bounty Arctic Watershed Observatory for the summer season at hourly, daily, and weekly timescales

	Full dataset			Partial dataset		
	Flux	RMSE	R^2	Flux	RMSE	R^2
Hourly	NEE	0.28	0.93	NEE	0.34	0.88
	ER	0.29	0.46	ER	0.29	0.48
	GPP	0.31	0.89	GPP	0.33	0.87
Daily	NEE	0.31	0.74	NEE	0.23	0.77
	ER	0.36	0.47	ER	0.27	0.31
	GPP	0.32	0.38	GPP	0.24	0.46
Weekly	NEE	0.16	0.81	NEE	0.14	0.87
	ER	0.17	0.41	ER	0.17	0.59
	GPP	0.19	0.68	GPP	0.12	0.84

Note: For the partial dataset, the data from the pair of autochambers at the Goose watershed were excluded.

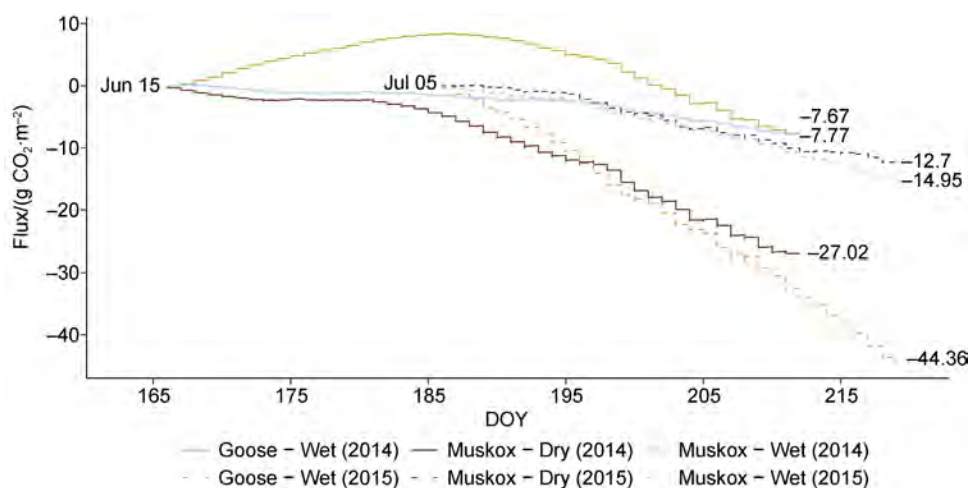


Figure 5 Cumulative net ecosystem exchange measured from three autochamber pairs at the Cape Bounty Arctic Watershed Observatory for the 2014 and 2015 summer seasons. DOY = Day of the Year.

In addition to evaluating the model using the 2014 observations not included in the training dataset, the model predictions were assessed using data from the autochamber pairs deployed in 2015. The model was run without soil moisture measurements as these were not collected in 2015. The data from the autochamber pair located at the Goose site were excluded given the large percentage of data points identified as outliers and removed at the filtering stage (37.2%). The exclusion of Goose data greatly improved model performance. The model fits for GPP and NEE had strong R^2 values (0.81 and 0.68, respectively), but ER was still poorly predicted ($R^2 = 0.34$). The RMSE was lowest for ER ($0.47 \mu\text{mol}\cdot\text{m}^{-2}\cdot\text{s}^{-1}$) and higher for NEE ($0.76 \mu\text{mol}\cdot\text{m}^{-2}\cdot\text{s}^{-1}$) and GPP ($0.57 \mu\text{mol}\cdot\text{m}^{-2}\cdot\text{s}^{-1}$).

A further analysis was performed to investigate the importance of the predictive variables at different temporal scales. The hourly data were aggregated into daily and weekly timescales. For daily values, the mean of the hourly fluxes for each date was used while the weekly values were calculated using a seven-day moving average. Model predictive power (R^2) was generally highest at the hourly scale and lowest at the daily scale, while uncertainty (RMSE) was lowest at the weekly scale and highest at the daily scale. The model continued to perform better for predicting NEE and GPP compared to ER at all temporal scales (Table 3).

At the hourly scale, NEE and GPP were strongly influenced by PAR, with all other variables having a relatively low importance (Figure 6). By contrast, multiple variables showed similar importance for predicting ER at the hourly scale. However, soil temperature (5 cm depth) emerged as the most important variable at the daily and weekly time scales. Meanwhile, the influence of air temperature on ER decreased at daily and weekly scales. For all three fluxes, the importance of PAR decreased at coarser temporal scales, while the importance of soil temperature increased. Soil moisture

and soil moisture classes became more important variables with aggregation, especially for modelling respiration. The importance of Julian Day as a variable for modelling NEE and GPP was high at the daily scale and moderate at the weekly scale. The importance of Julian Day for predicting respiration decreased from the hourly to daily scales.

3.5 Respiration models

Alternative regression models for ER were compared to the RF model (Table 4). The models were run without data from the Goose site, as its inclusion significantly reduced model performance. The models were computed with both soil and air temperature; results were similar, so the more complete air temperature measurements from Main Met were used for this analysis. The models were also tested with one- and two-hour time lags in the temperature readings since the respiratory response to temperature changes is often delayed, but this reduced model performance. All models had low R^2 values (0.10 – 0.30) and RMSE of $0.30 - 0.40 \mu\text{mol}\cdot\text{m}^{-2}\cdot\text{s}^{-1}$. The residuals for the models were generally evenly distributed, indicating a lack of bias. Based on the Akaike Information Criterion (AIC), the top performing models were the soil water content (SWC) modulated logistic model and the time-varying Q10 model, followed closely by the simple linear regression (Table 4).

3.6 Static chambers

For the static chamber measurements, soil moisture readings of the top 7 cm confirmed wet and dry designations. Wet and dry sites had significantly different soil moisture levels over the entire growing season with an average of 77% moisture content at wet sites compared to 37% at dry sites (Wilcoxon $p < 0.001$). At the plot level, wet sites had almost exclusively higher soil moisture levels than dry sites throughout the measurement period.

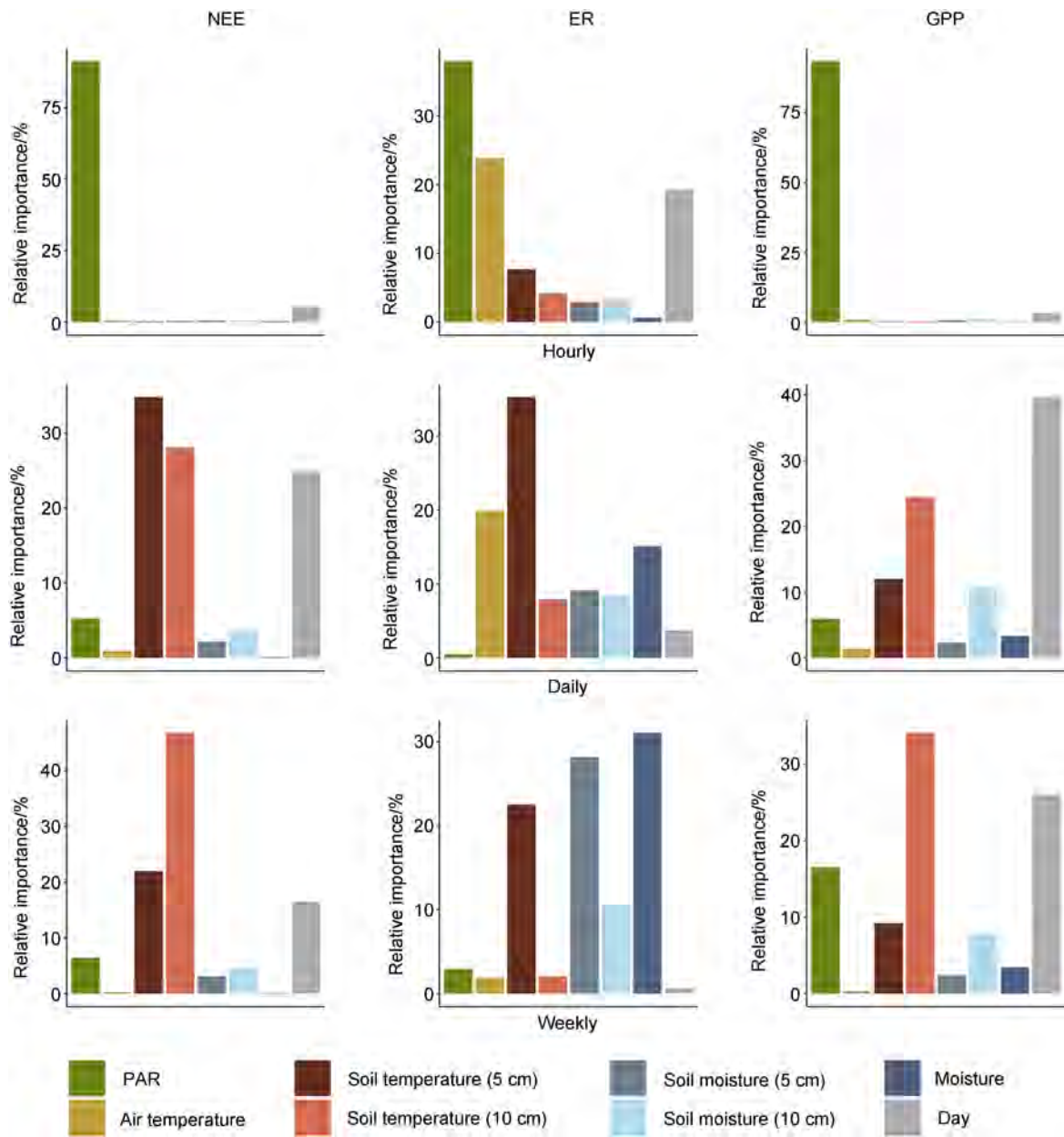


Figure 6 Relative variable importance for predicting carbon dioxide fluxes at hourly (top), daily (middle), and weekly (bottom) temporal scales using Random Forest regression on flux data collected from three autochamber sites at the Cape Bounty Arctic Watershed Observatory in the 2014 summer season.

As with the autochamber measurements, NEE flux rates from static chambers (Supplementary Figure 2) differed significantly between wet ($-0.047 \pm 0.071 \mu\text{mol}\cdot\text{m}^{-2}\cdot\text{s}^{-1}$) and dry sites ($0.05 \pm 0.42 \mu\text{mol}\cdot\text{m}^{-2}\cdot\text{s}^{-1}$) (Wilcoxon $p < 0.001$). Positive NEE for dry sites showed that dry sites were an overall source for the 2014 summer season. This was contrary to the autochamber results, which indicated that wet and dry sites were net CO_2 sinks. A significant difference was also observed between the rate of GPP which was higher at wet sites compared dry sites (Wilcoxon $p < 0.001$). However, unlike the autochamber results, ER did not differ significantly between the moisture

regimes (Wilcoxon $p > 0.1$).

4 Discussion

Microclimatic and topographic differences in High Arctic landscapes lead to significant variability in soil moisture regimes, even within vegetation types (Sjögersten et al., 2006; Liu and Treitz, 2016). Given the large amount of carbon currently stored in Arctic permafrost and the rapid rate of climate change in this region, predicting changes in net carbon storage will require a greater understanding of the impact of hydrological variability on CO_2 exchange

Table 4 Regression models and model performance for hourly ecosystem respiration from autochamber measurements at the Cape Bounty Arctic Watershed Observatory for the 2014 and 2015 summer seasons (adapted from Richardson et al. (2006))

Model	Equation	AIC	References
Linear	$\theta_1 + \theta_2 T$	997	
Arrhenius	$\theta_1 e^{\left(\frac{\theta_2}{283.15K} \frac{1-283.15}{T}\right)}$	1008	Lloyd and Taylor (1994); Sjögersten and Wookey (2002)
Basic Q10	$\theta_1 \theta_2 \left(\frac{T-10}{10}\right)$	1009	Black et al. (1996)
Temperature-Varying Q10	$\theta_1 (\theta_2 + \theta_3 T) \left(\frac{T-10}{10}\right)$	1001	Tjoelker et al. (2001)
Time-Varying Q10	$\theta_1 (\theta_2 + \theta_3 \sin(JD_\pi) + \theta_4 \cos(JD_\pi)) \left(\frac{T-10}{10}\right)$	866	
SWC Modulated Q10	$\theta_1 \theta_2 \left(\frac{T-10}{10}\right) \times \frac{SWC}{SWC + \theta_3} \times \frac{\theta_4}{SWC + \theta_4}$	1188	Bunnell et al. (1977); Carlyle (1988)
Lloyd and Taylor	$\theta_1 e^{308.56\left(\frac{1}{56.02} - \frac{1}{T-227.15}\right)}$	1000	Soegaard and Nordstroem (1999); Lloyd (2001)
Logistic	$\frac{\theta_1}{1 + e^{(\theta_2 - \theta_3 T)}}$	1000	
SWC Modulated Logistic	$\frac{\theta_1}{1 + e^{(\theta_2 - \theta_3 T)}} \times \frac{SWC}{SWC + \theta_4} \times \frac{\theta_5}{SWC + \theta_5}$	941	Sharp et al. (2013)

Notes: R = gas constant; $JD_\pi = 2 \times \pi \times$ Julian Day; SWC = soil water content (%); T = air temperature (in °C or K)

processes at high latitudes. To this end, wet sedge vegetation at the CBAWO was partitioned into wet and dry sites using satellite-based methods and confirmed by *in situ* soil measurements (Liu and Treitz, 2016). Our results indicate differences in CO₂ flux rates between wet and dry sedge meadows. Based on Random Forest modelling and various non-linear regressions, we suggest that the variation is primarily attributable to the indirect influence of soil moisture regimes on vegetation and on the temperature response of CO₂ exchange processes.

4.1 Soil moisture and soil temperature

Soil temperatures were warmer at dry sites in both years. Temperature measurements were taken within the top 10 cm of soil and thus reflected hourly changes in air temperature. The higher heat capacity and higher thermal conductivity of wet soils compared to dry soils likely combined to generate warmer average soil temperatures at dry compared to wet sites. This finding supports similar observations at the CBAWO (Wagner et al., 2019) and other High Arctic sites (Sjögersten et al., 2006; Elberling, 2007). However, opposite trends have been observed at some sites in Alaska (McEwing et al., 2015; Juszak et al., 2016), and differences in microtopography and sensor depth can also substantially influence soil temperature readings (Klene et al., 2001). The impact of soil moisture on soil temperature may be important when considering the influence of moisture differences on CO₂ exchange among wet sedge communities.

4.2 Autochamber CO₂ fluxes

Flux measurements from the three autochamber sites indicate that wet sedge communities are net CO₂ sinks in the High Arctic. Cumulative NEE was negative for all sites

across both years (−7.67 to −44.36 g C·m^{−2}). Braybrook (2020) reported similar interannual ranges for growing season cumulative NEE at the CBAWO (−46.01 to 11.25 g C·m^{−2}). Mean and median values and amplitudes of the three flux rates (NEE, ER, and GPP) are also comparable to other Arctic CO₂ exchange measurements (Dagg and Lafleur, 2011; Atkinson et al., 2020). The autochamber results support the need for distinguishing between moisture regimes in wet sedge meadows (wet and dry) when modeling landscape-scale CO₂ fluxes. All fluxes except GPP in 2015 differed significantly between moisture regimes (Wilcoxon $p < 0.01$). This is consistent with previous findings that ER generally varies more strongly with soil moisture compared to GPP (Marchand et al., 2005; Natali et al., 2015). In 2014, the wet sites had overall lower (less negative) NEE compared to the dry site. Increased water availability has previously been shown to enhance respiration (Illeris et al., 2003; Christiansen et al., 2012; Emmerton et al., 2016) which could explain the lower rates of NEE at wet sites compared to dry sites in 2014. By contrast, in 2015, the wet sites had larger NEE values (more uptake) compared to the dry site. The 2015 growing season received substantially more precipitation than the average of the previous ten summers. It is possible that higher precipitation led to increased soil moisture and higher respiration in 2015 at dry sites as observed by Elmendorf et al. (2016) in High Arctic polar semi-desert sites. Sjoergersen et al. (2006) also suggest that ER is limited under anaerobic moisture conditions but stimulated at drier sites by increased carbon availability. Indeed, the results indicate that ER increased at dry sites from 2014 ($0.50 \pm 0.38 \mu\text{mol}\cdot\text{m}^{-2}\cdot\text{s}^{-1}$) to 2015 ($1.08 \pm 0.41 \mu\text{mol}\cdot\text{m}^{-2}\cdot\text{s}^{-1}$) while remaining essentially unchanged at wet sites (which were likely close to saturation).

4.3 Static chamber CO₂ fluxes

Over a larger area, NEE and GPP were significantly greater at wet sites compared to dry sites (Wilcoxon $p < 0.001$), while ER did not differ significantly between the moisture classes (Wilcoxon $p > 0.1$). In contrast to autochamber results, static chamber measurements showed that dry sites were an overall CO₂ source for the 2014 summer season. This may be attributed to lower sampling frequency or timing of sampling compared to the autochambers. Additionally, NDVI was significantly greater for wet compared to dry sites (Wilcoxon $p < 0.01$) which is indicative of increased biomass. Both percent cover and biomass correlate positively with soil moisture within wet sedge meadows (Atkinson and Treitz, 2013). This would account for the increased productivity of wet sites compared to dry sites. Overall, these spatially extensive measurements confirmed the significant difference in CO₂ exchange processes across soil moisture regimes in High Arctic wet sedge communities.

4.4 RF flux modelling

To explore the controls on CO₂ fluxes in wet sedge communities, autochamber data were modelled using an RF algorithm. Machine learning algorithms such as RF are increasingly being used to model carbon fluxes, including in Arctic ecosystems, due to their predictive power and robustness against overprediction (Bond-Lamberty et al., 2012; López-Blanco et al., 2017; Zhou et al., 2019). The final RF models accurately modeled hourly NEE and GPP, and adequately simulated ER based on validation with out-of-bag observations and a separate 2015 dataset. There was a slight bias in the residuals of hourly NEE (Supplementary Figure 1), likely due to data outliers not captured by the filtering for the individual chambers; but that appeared when the data were aggregated (i.e. when NEE is calculated from GPP and ER). It is important to note that 2015 data were collected at the same site as 2014 measurements which may have caused a slight overestimation of predictive performance. When simulating 2015 ER, amplitude peaks on both top and bottom of the diel signature were underestimated (Supplementary Figure 1). The poor performance of ER compared to other fluxes may simply be a result of the robustness of the data collected by the transparent autochambers compared to the opaque ones (i.e., many more outliers were identified for fluxes measured at opaque chambers). It could also be that the environmental variables included in the analysis are better suited to predict GPP and NEE than ER (see importance of PAR below). The model performance is similar to other attempts to model CO₂ fluxes using machine learning at lower latitudes (Dou et al., 2018; Zhou et al., 2019), indicating that these emerging modelling techniques can be used to understand carbon cycling processes in the High Arctic.

Based on RF models of hourly, daily, and weekly data,

our results show that different controlling factors operate at different temporal scales. At the hourly scale, PAR was the most influential variable for all three fluxes. PAR is a strong control of GPP, and by extension NEE, due to its direct impact on photosynthesis (Oechel et al., 2014). However, our results differ in that PAR is typically not found to have a strong relationship with ER compared to temperature at the hourly scale (López-Blanco et al., 2017; Braybrook, 2020). It is possible that PAR was driving GPP which in turn stimulated ER (Shaver et al., 2007). More likely, PAR indirectly influenced ER through a warming effect as suggested by Oechel et al. (2007). The importance of PAR decreased significantly for models of daily and weekly fluxes. Instead, Julian Day and soil temperature became the top variables for NEE and GPP. Julian Day can be regarded as an integrated measure of seasonal changes (e.g., solar radiation, temperature, day length) so it is not surprising that it serves as an important variable for modelling of NEE and GPP at coarser timescales. The supersedence of PAR by temperature in terms of variable importance as temporal aggregation increases has also been observed in the Low Arctic and other ecosystems (Ouyang et al., 2014; López-Blanco et al., 2017; Montagnani et al., 2018), suggesting that temperature is a more important control over the CO₂ balance of High Arctic ecosystems at coarser temporal scales.

Soil moisture measurements had little importance across all fluxes and timescales except for ER at the weekly scale. At this scale, the averaged instantaneous measurements were simply representing the moisture classes, and the impact of moisture on ER was due to differences between the two moisture regimes (e.g., vegetation, temperature) rather than a direct impact of soil moisture. The impact of soil moisture on net CO₂ exchange remained low even at the weekly scale. Instead, NEE appeared to be controlled by the temperature response of GPP (Figure 6). Overall, the results indicate that soil moisture may be more relevant as a variable when considering long-term variation in CO₂ exchange through impacts on vegetation and temperature regimes rather than acting as an instantaneous control of fluxes, particularly in these wet ecosystems.

NDVI was also evaluated as a predictor for CO₂ fluxes. The model performance was reduced by the inclusion of NDVI at all timescales. Several past studies have incorporated NDVI or Leaf Area Index (approximated from NDVI) into flux models (Shaver et al., 2007; Atkinson et al., 2020). However, these studies were carried out over larger spatiotemporal scales. NDVI varies on a seasonal or annual timescale, or across a larger area (i.e., across different vegetation types), so while it could be relevant for predicting fluxes at larger scales, it does not have a strong relationship with short-term, local variation in CO₂ exchange (i.e., for a single vegetation type within one year).

4.5 Respiration models

Given the limitations of the RF model for predicting ER, we tested the utility of several non-linear ER models (Table 4). Although comparison of predicted vs. observed results produced unbiased residual plots and slopes close to 1.0, the underestimation of flux amplitude present in RF models was also apparent with these non-linear models. Basic Arrhenius, Q10, and Lloyd and Taylor models performed poorly compared to a simple linear model according to AIC values. Although these models are commonly used to predict ER (Richardson et al., 2006), they have seldom successfully modelled ER at high latitudes. For example, Wilkman et al. (2018) found R^2 values of 0.05 to 0.68 for Q10 models of hourly ER across several ecosystem types in the Alaskan Arctic tundra. The top performing model was a time-varying Q10 model adapted from Richardson et al. (2006) (Table 4). Though their work was not conducted at high latitudes, Richardson et al. (2006) also found that the time-varying Q10 model consistently outperformed a temperature-dependent one. They suggest that the relationship between temperature and Q10 is oversimplified in the temperature-dependent Q10 model (which relies on an implicit linear relationship) and that it is better captured by the time-varying Q10 model. Based on AIC values, the second-best performing model was the SWC modulated logistic model. Sharp et al. (2013) also found that a soil moisture-modulated logistic model outperformed most simple temperature-dependent exponential models of ER in the High Arctic. Previous research has indicated that the temperature response of ER in the Arctic is highly dependent on soil moisture (Huemmrich et al., 2010; Dagg and Lafleur, 2011). Our results indicate generally poor performance of strictly temperature-based ER models at High Arctic sites and suggest that soil moisture is an important control in these ecosystems. Furthermore, based on our results, the influence of soil moisture on ER is likely manifested through differences in vegetation and temperature responses rather than an instantaneous effect. Future work will explore the temperature sensitivity of ER in multiple vegetation types with different soil moisture regimes.

Given the ongoing changes in High Arctic climate and their potential impacts on the carbon cycle, our results have important implications. CO₂ exchange processes differed in the two moisture classes within wet sedge communities. Significant differences were observed in flux rates between wet and dry designated wet sedge communities at a high temporal frequency (autochambers) and across a larger spatial scale (static chambers). The wet and dry areas also responded differently to temperature variability between the two years. Through RF modelling, our results indicate that short term (hourly to daily) changes in soil moisture have little to no impact on flux rates. However, on a larger timescale, the moisture classes were shown to impact respiration. Lastly, our results indicate that frequently used

temperature-based models may be inadequate for modelling High Arctic ER. The models could be improved by adding soil moisture as an indirect control (e.g., temperature, vegetation distribution) on CO₂ fluxes. Overall, our results indicate that CO₂ fluxes are not strongly influenced by instantaneous changes in soil moisture but rather by the heterogeneity in vegetation and abiotic regimes represented by moisture gradients within wet sedge communities. This is important in light of recent results indicating an increased importance of rainfall as part of the hydrological regime in the High Arctic (Beel et al., 2020). Shifts in vegetation abundance and community composition have also been recorded (Sim et al., 2019; Ravolainen et al., 2020), which may lead to an increase in the extent of wet sedge meadows (Wagner et al., 2019). These changes are especially relevant given our findings regarding the impact of moisture regimes on CO₂ exchange processes in wet sedge meadows and their current function as strong CO₂ sinks.

5 Conclusion

Carbon dioxide exchange rates have been shown to vary strongly across moisture gradients in the High Arctic (Oberbauer et al., 2007; Wagner et al., 2019); however, few studies have examined the impacts of moisture variability within a single vegetation type. Our results indicate that variation in soil moisture regimes, specifically within vegetation communities, needs to be considered when analysing and predicting changes in the net CO₂ balance of Arctic ecosystems. We have shown that the impact of soil moisture on CO₂ fluxes is primarily indirect through its influence on vegetation (e.g., plant cover, biomass) and on the temperature response of CO₂ exchange processes. Direct limitation or stimulation of fluxes through instantaneous changes in soil moisture levels was not observed. Our results also suggest that commonly-used models of ER are not adequate for predicting respiration at this High Arctic site. These models could potentially benefit from the incorporation of additional variables, including soil moisture regimes across the landscape. Climate change is already altering soil moisture regimes across high latitudes, and rainfall is expected to continue to increase (Liston and Hiemstra, 2011; Bintanja and Andry, 2017). Our results indicate that this could have a strong impact on the carbon balance of the High Arctic, and that the impact may vary depending on how changes to soil moisture interact with changes to other environmental variables.

Acknowledgements This research would not have been possible without financial and logistical support from ArcticNet NCE, the Natural Sciences and Engineering Research Council, Natural Resources Canada (Polar Continental Shelf Program), the Northern Scientific Training Program, and Queen's University. The authors thank the three anonymous reviewers, and Associate Editor, Dr. Steve Coulson for their constructive comments and suggestions.

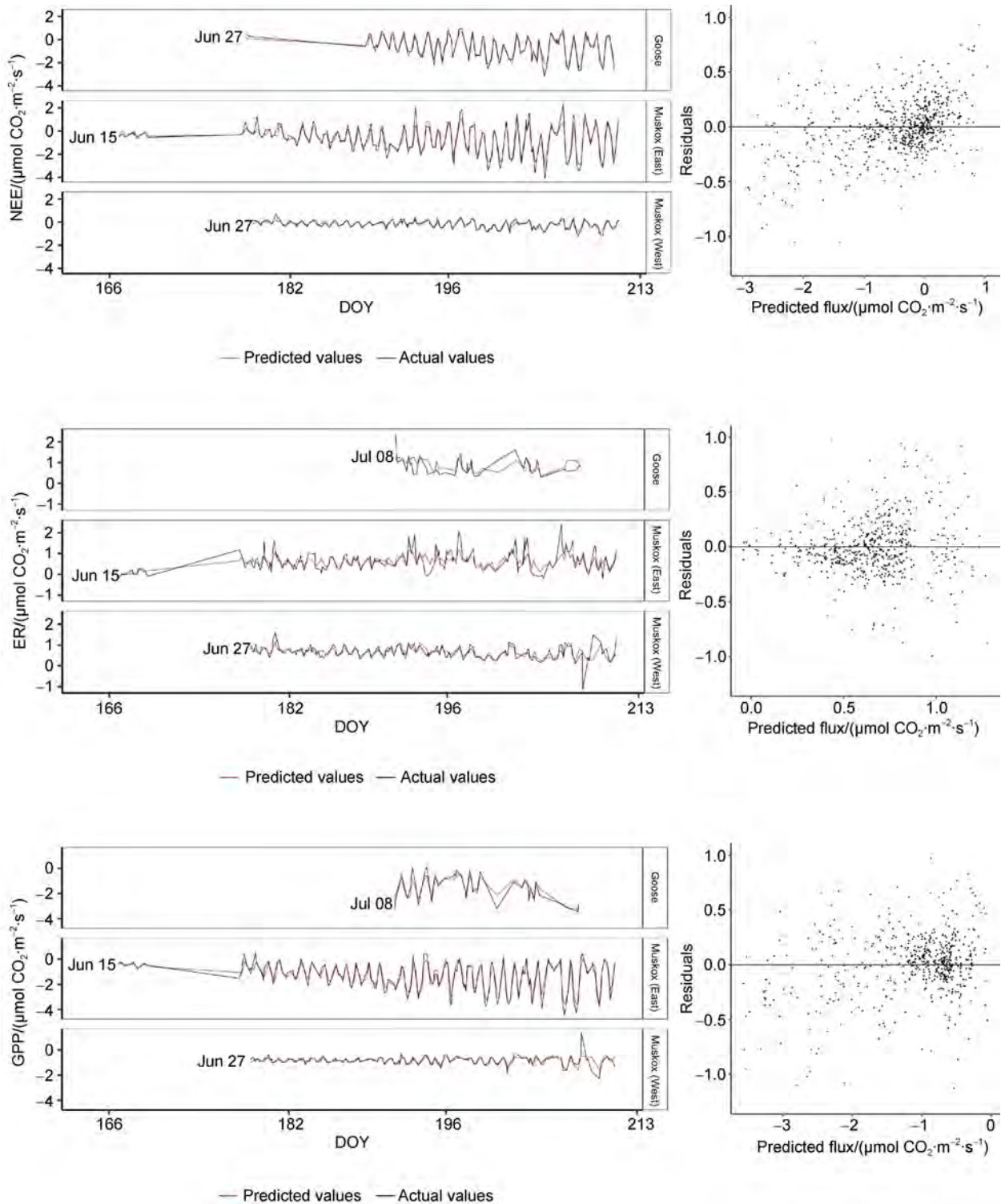
References

- Arnold J G, Kiniry J R, Srinivasan R, et al. 2012. Soil water assessment tool: input/output documentation. Texas Water Resources Institute.
- Atkinson D M, Hung J K Y, Gregory F M, et al. 2020. High spatial resolution remote sensing models for landscape-scale CO₂ exchange in the Canadian Arctic. *Arct Antarct Alp Res*, 52(1): 248-263, doi:10.1080/15230430.2020.1750805.
- Atkinson D M, Treitz P. 2012. Arctic ecological classifications derived from vegetation community and satellite spectral data. *Remote Sens*, 4(12): 3948-3971, doi:10.3390/rs4123948.
- Beamish A L, Neil A, Wagner I, et al. 2014. Short-term impacts of active layer detachments on carbon exchange in a High Arctic ecosystem, Cape Bounty, Nunavut, Canada. *Polar Biol*, 37(10): 1459-1468, doi:10.1007/s00300-014-1536-4.
- Beamish A L, Reynolds M K, Epstein H, et al. 2020. Recent trends and remaining challenges for optical remote sensing of Arctic tundra vegetation: a review and outlook. *Remote Sens Environ*, 246: 111872, doi:10.1016/j.rse.2020.111872.
- Beel C R, Lamoureux S F, Orwin J F, et al. 2020. Differential impact of thermal and physical permafrost disturbances on High Arctic dissolved and particulate fluvial fluxes. *Sci Rep*, 10(1): 11836, doi:10.1038/s41598-020-68824-3.
- Bintanja R, Andry O. 2017. Towards a rain-dominated Arctic. *Nat Clim Chang*, 7(4): 263-267, doi:10.1038/nclimate3240.
- Bintanja R, Selten F M. 2014. Future increases in Arctic precipitation linked to local evaporation and sea-ice retreat. *Nature*, 509(7501): 479-482. doi:10.1038/nature13259.
- Black T A, den Hartog G, Neumann H H, et al. 1996. Annual cycles of water vapour and carbon dioxide fluxes in and above a boreal aspen forest. *Glob Chang Biol*, 2(3): 219-229, doi: 10.1111/j.1365-2486.1996.tb00074.x.
- Bond-Lamberty B, Bunn A G, Thomson A M. 2012. Multi-year lags between forest browning and soil respiration at high northern latitudes. *PLoS One*, 7(11): e50441, doi:10.1371/journal.pone.0050441.
- Box J E, Colgan W T, Christensen T R, et al. 2019. Key indicators of Arctic climate change: 1971-2017. *Environ Res Lett*, 14(4): 045010, doi: 10.1088/1748-9326/aafc1b.
- Braybrook C A. 2020. Impact of environmental variability on net ecosystem exchange from 2008-2018 at a High Arctic mesic tundra site. M.S. thesis, Kingston, Ontario: Queen's University.
- Bunnell F L, Tait D E N, Flanagan P W, et al. 1977. Microbial respiration and substrate weight loss—I. *Soil Biol and Biochem*, 9(1): 33-40, doi: 10.1016/0038-0717(77)90058-x.
- Campbell T K F, Lantz T C, Fraser R H, et al. 2021. High Arctic vegetation change mediated by hydrological conditions. *Ecosystems*, 24(1): 106-121, doi:10.1007/s10021-020-00506-7.
- Cannone N, Ponti S, Christiansen H H, et al. 2019. Effects of active layer seasonal dynamics and plant phenology on CO₂ land-atmosphere fluxes at polygonal tundra in the High Arctic, Svalbard. *CATENA*, 174: 142-153, doi: 10.1016/j.catena.2018.11.013.
- Carlyle J C, Than U B. 1988. Abiotic controls of soil respiration beneath an eighteen-year-old *Pinus radiata* stand in south-eastern Australia. *J Ecol*, 76(3): 654-662, doi:10.2307/2260565.
- Christiansen C T, Svendsen S H, Schmidt N M, et al. 2012. High Arctic heath soil respiration and biogeochemical dynamics during summer and autumn freeze-in-effects of long-term enhanced water and nutrient supply. *Glob Chang Biol*, 18(10): 3224-3236, doi: 10.1111/j.1365-2486.2012.02770.x.
- Dagg J, Lafleur P. 2011. Vegetation community, foliar nitrogen, and temperature effects on tundra CO₂ exchange across a soil moisture gradient. *Arct Antarct Alp Res*, 43(2): 189-197, doi: 10.1657/1938-4246-43.2.189.
- Davy R, Chen L L, Hanna E. 2018. Arctic amplification metrics. *Int J Climatol*, 38(12): 4384-4394, doi:10.1002/joc.5675.
- Dou X M, Yang Y G, Luo J H. 2018. Estimating forest carbon fluxes using machine learning techniques based on eddy covariance measurements. *Sustainability*, 10(1): 203, doi:10.3390/su10010203.
- Elberling B. 2007. Annual soil CO₂ effluxes in the High Arctic: The role of snow thickness and vegetation type. *Soil Biol Biochem*, 39(2): 646-654, doi:10.1016/j.soilbio.2006.09.017.
- Elmendorf S C, Henry G H R, Hollister R D, et al. 2012. Global assessment of experimental climate warming on tundra vegetation: heterogeneity over space and time. *Ecol Lett*, 15(2): 164-175, doi:10.1111/j.1461-0248.2011.01716.x.
- Emmerton C A, St. Louis V L, Humphreys E R, et al. 2016. Net ecosystem exchange of CO₂ with rapidly changing High Arctic landscapes. *Glob Chang Biol*, 22(3): 1185-1200, doi: 10.1111/gcb.13064.
- Gitelson A A, Kaufman Y J, Merzlyak M N. 1996. Use of a green channel in remote sensing of global vegetation from EOS-MODIS. *Remote Sens Environ*, 58(3): 289-298, doi: 10.1016/S0034-4257(96)00072-7.
- Hastie T, Tibshirani R, Friedman J. 2017. The elements of statistical learning: data mining, inference, and prediction, 2nd edn. New York: Springer, 587-605.
- Heinemeyer A, Di Bene C, Lloyd A R, et al. 2011. Soil respiration: Implications of the plant-soil continuum and respiration chamber collar-insertion depth on measurement and modelling of soil CO₂ efflux rates in three ecosystems. *Eur J Soil Sci*, 62(1): 82-94, doi:10.1111/j.1365-2389.2010.01331.x.
- Hill G B, Henry G H R. 2011. Responses of High Arctic wet sedge tundra to climate warming since 1980. *Glob Chang Biol*, 17(1): 276-287, doi:10.1111/j.1365-2486.2010.02244.x.
- Hobbie J E, Shaver G R, Rastetter E B, et al. 2017. Ecosystem responses to climate change at a Low Arctic and a High Arctic long-term research site. *Ambio*, 46(1): 160-173, doi: 10.1007/s13280-016-0870-x.
- Hothorn T, Hornik K, Strobl C, et al. 2020. Package "party." in CRAN.
- Hothorn T, Hornik K, Zeileis A. 2006. Unbiased recursive partitioning: A conditional inference framework. *J Comput Graph Stat*, 15(3): 651-674, doi:10.1198/106186006X133933.
- Huemrich K F, Kinoshita G, Gamon J A, et al. 2010. Tundra carbon balance under varying temperature and moisture regimes. *J Geophys Res: Biogeosciences*, 115(G4): G00I02, doi:10.1029/2009jg001237.
- Hugelius G, Strauss J, Zubrzycki S, et al. 2014. Estimated stocks of circumpolar permafrost carbon with quantified uncertainty ranges and identified data gaps. *Biogeosciences*, 11(23): 6573-6593, doi:10.5194/bg-11-6573-2014.
- Hung J K Y, Treitz P. 2020. Environmental land-cover classification for integrated watershed studies: Cape Bounty, Melville Island, Nunavut. *Arct Sci*, 6(4): 404-422, doi:10.1139/as-2019-0029.
- Illeris A L, Michelsen A, Jonasson S. 2003. Soil plus root respiration and microbial biomass following water, nitrogen, and phosphorus application at a High Arctic semi desert. *Biogeochemistry*, 65(1):

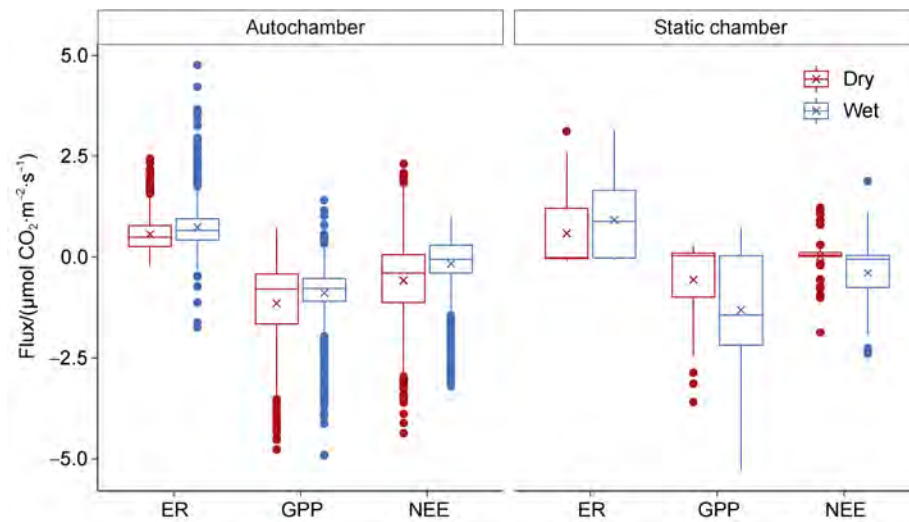
- 15-29, doi:10.1023/A:1026034523499.
- IPCC. 2019. Polar Regions/IPCC. IPCC special report on the ocean and cryosphere in a changing climate, Vol. 3, Issue Suppl., 203-320, doi:10.1016/S1366-7017(01)00066-6.
- Johnson L C, Shaver G R, Cades D H, et al. 2000. Plant carbon-nutrient interactions control CO₂ exchange in Alaskan wet sedge tundra ecosystems. *Ecology*, 81(2): 453-469, doi: 10.1890/0012-9658(2000)081[0453:PCNICC]2.0.CO;2.
- Ju J C, Masek J G. 2016. The vegetation greenness trend in Canada and US Alaska from 1984-2012 Landsat data. *Remote Sens Environ*, 176: 1-16, doi: 10.1016/j.rse.2016.01.001.
- Juszak I, Eugster W, Heijmans M M P D, et al. 2016. Contrasting radiation and soil heat fluxes in Arctic shrub and wet sedge tundra. *Biogeosciences*, 13(13): 4049-4064, doi:10.5194/bg-13-4049-2016.
- Kankaanpää T, Skov K, Abrego N, et al. 2018. Spatiotemporal snowmelt patterns within a High Arctic landscape, with implications for flora and fauna. *Arct Antarct Alp Res*, 50(1): e1415624, doi: 10.1080/15230430.2017.1415624.
- Klene A E, Nelson F E, Shiklomanov N I, et al. 2001. The *n*-factor in natural landscapes: variability of air and soil-surface temperatures, Kuparuk River Basin, Alaska, U.S.A. *Arct Antarct Alp Res*, 33(2): 140-148, doi:10.1080/15230430.2001.12003416.
- Kuhn M, Wing J, Weston S, et al. 2020. Package 'caret.' in CRAN. [2020-03-20]. <https://github.com/topepo/caret/issues>.
- Kutzbach L, Schneider J, Sachs T, et al. 2007. CO₂ flux determination by closed-chamber methods can be seriously biased by inappropriate application of linear regression. *J Geo Res*, 4(6): 1005-1025, doi:10.5194/bg-4-1005-2007.
- Kwon H J, Oechel W C, Zulueta R C, et al. 2006. Effects of climate variability on carbon sequestration among adjacent wet sedge tundra and moist tussock tundra ecosystems. *J Geophys Res: Biogeosciences*, 111(G3): G03014, doi:10.1029/2005JG000036.
- Lavoie M, Mack M C, Schuur E A G. 2011. Effects of elevated nitrogen and temperature on carbon and nitrogen dynamics in Alaskan Arctic and boreal soils. *J Geophys Res: Biogeosciences*, 116(G3): G03013, doi:10.1029/2010JG001629.
- Leys C, Ley C, Klein O, et al. 2013. Detecting outliers: Do not use standard deviation around the mean, use absolute deviation around the median. *J Exp Soc Psych*, 49(4): 764-766, doi:10.1016/j.jesp.2013.03.013.
- Liston G E, Hiemstra C A. 2011. The changing cryosphere: Pan-Arctic snow trends (1979-2009). *J Clim*, 24(21): 5691-5712, doi:10.1175/jcli-d-11-00081.1.
- Liu N, Treitz P. 2016. Modelling High Arctic percent vegetation cover using field digital images and high resolution satellite data. *Int J Appl Earth Obs Geoinf*, 52: 445-456, doi:10.1016/j.jag.2016.06.023.
- Lloyd C R. 2001. On the physical controls of the carbon dioxide balance at a High Arctic site in Svalbard. *Theor Appl Climatol*, 70(1-4): 167-182, doi:10.1007/s007040170013.
- Lloyd J, Taylor J A. 1994. On the temperature dependence of soil respiration. *Funct Ecol*, 8(3): 315-323, doi:10.2307/2389824.
- López-Blanco E, Lund M, Williams M, et al. 2017. Exchange of CO₂ in Arctic tundra: impacts of meteorological variations and biological disturbance. *Biogeosciences*, 14(19): 4467-4483, doi:10.5194/bg-14-4467-2017.
- Lüers J, Westermann S, Piel K, et al. 2014. Annual CO₂ budget and seasonal CO₂ exchange signals at a High Arctic permafrost site on Spitsbergen, Svalbard Archipelago. *Biogeosciences*, 11: 6307-6322, doi: 10.5194/bg-11-6307-2014.
- Marchand F L, Mertens S, Kockelbergh F, et al. 2005. Performance of High Arctic tundra plants improved during but deteriorated after exposure to a simulated extreme temperature event. *Glob Chang Biol*, 11(12): 2078-2089, doi:10.1111/j.1365-2486.2005.01046.x.
- McEwing K R, Fisher J P, Zona D. 2015. Environmental and vegetation controls on the spatial variability of CH₄ emission from wet-sedge and tussock tundra ecosystems in the Arctic. *Plant Soil*, 388(1-2): 37-52, doi:10.1007/s11104-014-2377-1.
- Mekonnen Z A, Riley W J, Grant R F. 2018. Accelerated nutrient cycling and increased light competition will lead to 21st century shrub expansion in north American Arctic tundra. *J Geophys Res: Biogeosciences*, 123(5): 1683-1701, doi:10.1029/2017JG004319.
- Montagnani L, Zanutelli D, Tagliavini M, et al. 2018. Timescale effects on the environmental control of carbon and water fluxes of an apple orchard. *Ecol Evol*, 8(1): 416-434, doi:10.1002/ece3.3633.
- Mudryk L R, Derksen C, Howell S, et al. 2018. Canadian snow and sea ice: Historical trends and projections. *Cryosphere*, 12(4): 1157-1176, doi:10.5194/tc-12-1157-2018.
- Myers-Smith I H, Grabowski M M, Thomas H J D, et al. 2019. Eighteen years of ecological monitoring reveals multiple lines of evidence for tundra vegetation change. *Ecol Monogr*, 89(2): e01351, doi:10.1002/ecm.1351.
- Myers-Smith I H, Kerby J T, Phoenix G K, et al. 2020. Complexity revealed in the greening of the Arctic. *Nat Clim Chang*, 10(2): 106-117, doi:10.1038/s41558-019-0688-1.
- Natali S M, Schuur E A G, Mauritz M, et al. 2015. Permafrost thaw and soil moisture driving CO₂ and CH₄ release from upland tundra. *J Geophys Res: Biogeosciences*, 120(3): 525-537, doi:10.1002/2014JG002872.
- Natali S M, Schuur E A G, Webb E E, et al. 2014. Permafrost degradation stimulates carbon loss from experimentally warmed tundra. *Ecology*, 95(3): 602-608, doi:10.1890/13-0602.1.
- Oberbauer S F, Tweedie C E, Welker J M, et al. 2007. Tundra CO₂ fluxes in response to experimental warming across latitudinal and moisture gradients. *Ecol Monogr*, 77(2): 221-238, doi:10.1890/06-0649.
- Oechel W C, Laskowski C A, Burba G, et al. 2014. Annual patterns and budget of CO₂ flux in an Arctic tussock tundra ecosystem. *J Geophys Res: Biogeosciences*, 119(3): 323-339, doi:10.1002/2013JG002431.
- Ouyang Z, Chen J, Becker R, et al. 2014. Disentangling the confounding effects of PAR and air temperature on net ecosystem exchange at multiple time scales. *Ecol Complex*, 19: 46-58, doi:10.1016/j.ecocom.2014.04.005.
- Plaza C, Pegoraro E, Bracho R, et al. 2019. Direct observation of permafrost degradation and rapid soil carbon loss in tundra. *Nat Geosci*, 12(8): 627-631, doi:10.1038/s41561-019-0387-6.
- Ravn N R, Elberling B, Michelsen A. 2020. Arctic soil carbon turnover controlled by experimental snow addition, summer warming and shrub removal. *Soil Biol Biochem*, 142: 107698, doi: 10.1016/j.soilbio.2019.107698.
- Ravolainen V, Soininen E M, Jónsdóttir I S, et al. 2020. High Arctic ecosystem states: Conceptual models of vegetation change to guide long-term monitoring and research. *Ambio*, 49(3): 666-677, doi:10.1007/s13280-019-01310-x.

- Richardson A D, Braswell B H, Hollinger D Y, et al. 2006. Comparing simple respiration models for eddy flux and dynamic chamber data. *Agric For Meteorol*, 141(2-4): 219-234, doi: 10.1016/j.agrformet.2006.10.010.
- Savage K, Davidson E A, Richardson A D. 2008. A conceptual and practical approach to data analysis procedures for high-frequency soil measurements. *Funct Ecol*, 22(6): 1000-1007, doi:10.1111/j.1365-2435.2008.01414.x.
- Schuur E A G, Abbott B. 2011. Climate change: High risk of permafrost thaw. *Nature*, 480(7375): 32-33, doi:10.1038/480032a.
- Sharp E D, Sullivan P F, Steltzer H, et al. 2013. Complex carbon cycle responses to multi-level warming and supplemental summer rain in the High Arctic. *Glob Chang Biol*, 19(6): 1780-1792, doi:10.1111/gcb.12149.
- Shaver G R, Street L E, Rastetter E B, et al. 2007. Functional convergence in regulation of net CO₂ flux in heterogeneous tundra landscapes in Alaska and Sweden. *J Ecol*, 95(4): 802-817, doi: 10.1111/j.1365-2745.2007.01259.x.
- Sim T G, Swindles G T, Morris P J, et al. 2019. Pathways for ecological change in Canadian High Arctic wetlands under rapid twentieth century warming. *Geophys Res Lett*, 46(9): 4726-4737, doi:10.1029/2019GL082611.
- Sjögersten S, Wookey P A. 2002. Climatic and resource quality controls on soil respiration across a forest-tundra ecotone in Swedish Lapland. *Soil Biol Biochem*, 34(11): 1633-1646, doi: 10.1016/S0038-0717(02)00147-5.
- Sjögersten S, van der Wal R, Woodin S J. 2006. Small-scale hydrological variation determines landscape CO₂ fluxes in the High Arctic. *Biogeochemistry*, 80(3): 205-216, doi: 10.1007/s10533-006-9018-6.
- Soegaard H, Nordstroem C. 1999. Carbon dioxide exchange in a High-Arctic fen estimated by eddy covariance measurements and modelling. *Glob Chang Biol*, 5: 547-562.
- Strobl C, Boulesteix A L, Kneib T, et al. 2008. Conditional variable importance for random forests. *BMC Bioinformatics*, 9: 307, doi:10.1186/1471-2105-9-307.
- Tjoelker M G, Oleksyn J, Reich P B. 2001. Modelling respiration of vegetation: Evidence for a general temperature-dependent Q₁₀. *Glob Chang Biol*, 7(2): 223-230, doi: 10.1046/j.1365-2486.2001.00397.x
- Thompson D K, Woo M-K. 2009. Seasonal hydrochemistry of a High Arctic wetland complex. *Hydrol Process*, 23(10): 1397-1407, doi:10.1002/hyp.7271.
- Treat C C, Marushchak M E, Voigt C, et al. 2018. Tundra landscape heterogeneity, not interannual variability, controls the decadal regional carbon balance in the Western Russian Arctic. *Glob Chang Biol*, 24(11): 5188-5204, doi: 10.1111/gcb.14421.
- van der Wal R, Stien A. 2014. High-Arctic plants like it hot: a long-term investigation of between-year variability in plant biomass. *Ecology*, 95(12): 3414-3427, doi:10.1890/14-0533.1.
- Vihma T, Screen J, Tjernström M, et al. 2016. The atmospheric role in the Arctic water cycle: A review on processes, past and future changes, and their impacts. *J Geophys Res: Biogeosciences*, 121(3): 586-620, doi:10.1002/2015JG003132.
- Voigt C, Marushchak M E, Mastepanov M, et al. 2019. Ecosystem carbon response of an Arctic peatland to simulated permafrost thaw. *Glob Chang Biol*, 25(5): 1746-1764, doi: 10.1111/gcb.14574.
- Wagner I, Hung J K Y, Neil A, et al. 2019. Net greenhouse gas fluxes from three High Arctic plant communities along a moisture gradient. *Arct Sci*, 5(4): 185-201, doi:10.1139/as-2018-0018.
- Webber P J. 1978. Spatial and temporal variation of the vegetation and its production, Barrow, Alaska/Tieszen L L. *Ecological Studies*. New York, NY: Springer New York, 1978: 37-112. doi:10.1007/978-1-4612-6307-4_3.
- Welker J M, Fahnestock J T, Henry G H R, et al. 2004. CO₂ exchange in three Canadian High Arctic ecosystems: Response to long-term experimental warming. *Glob Chang Biol*, 10(12): 1981-1995, doi: 10.1111/j.1365-2486.2004.00857.x.
- Wilkman E, Zona D, Tang Y, et al. 2018. Temperature response of respiration across the heterogeneous landscape of the Alaskan Arctic tundra. *J Geophys Res: Biogeosciences*, 123(7): 2287-2302, doi:10.1029/2017JG004227.
- Woo M, Young K L, Brown L. 2006. High Arctic patchy wetlands: Hydrologic variability and their sustainability. *Phys Geogr*, 27(4): 297-307, doi: 10.2747/0272-3646.27.4.297.
- Wookey P A, Aerts R, Bardgett R D, et al. 2009. Ecosystem feedbacks and cascade processes: understanding their role in the responses of Arctic and alpine ecosystems to environmental change. *Glob Chang Biol*, 15(5): 1153-1172, doi:10.1111/j.1365-2486.2008.01801.x.
- Zhou Q, Fellows A, Flerchinger G N, et al. 2019. Examining interactions between and among predictors of net ecosystem exchange: A machine learning approach in a semi-arid landscape. *Sci Rep*, 9: 2222, doi:10.1038/s41598-019-38639-y.

Supplementary Figures



Supplementary Figure 1 Predicted and measured carbon dioxide fluxes, and associated residual plots using Random Forest regression modelling for a random subset of the 2014 data collected at three autochamber sites at the Cape Bounty Arctic Watershed Observatory for the summer season. DOY = Day of the Year.



Supplementary Figure 2 Comparison of median (line) and mean (cross) carbon dioxide fluxes measured at wet and dry wet sedge sites at CBAWO in the 2014 summer season (ER – Ecosystem Respiration, GPP – Gross Primary Productivity, NEE – Net Ecosystem Exchange). Measurements were collected hourly at three autochamber sites and approximately every 4 d at 24 static chamber sites. Static chamber fluxes were recorded between 1000 and 1600.